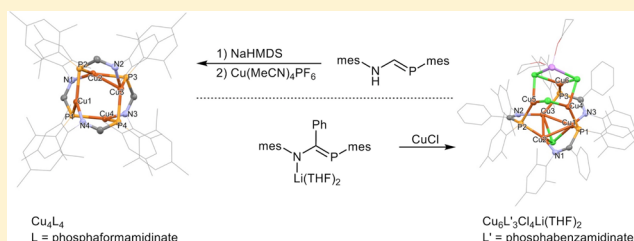


Multinuclear Cu(I) Clusters Featuring a New Triply Bridging Coordination Mode of Phosphaamidinate Ligands

Suresh C. Rathnayaka,[†] Sergey V. Lindeman,[‡] and Neal P. Mankad^{*,†}[†]Department of Chemistry, University of Illinois at Chicago, 845 West Taylor Street, Chicago, Illinois 60607, United States[‡]Department of Chemistry, Marquette University, 1414 W. Clybourn Street, Milwaukee, Wisconsin 53233, United States

Supporting Information

ABSTRACT: Phosphabenzamidine [mes-NH-C(Ph)=P-mes) (**1**) and phosphoformamidinate (mes-NH-CH=P-mes) (**4**) ligands have been synthesized and characterized. The conjugate bases of **1** and **4** coordinate by each bridging three Cu(I) ions, forming hexa- and tetranuclear clusters Cu₆[mes-N=C(Ph)-P-mes]₃Cl₄Li(THF)₂ (**3**) and Cu₄[mes-N=CH-P-mes]₄ (**5**), respectively. Both clusters have been fully characterized using ¹H NMR, ³¹P NMR, and X-ray crystallography. Complexes **3** and **5** exhibit a previously unknown coordination mode of phosphaamidinates, which are far less studied than their well-known amidinate counterparts



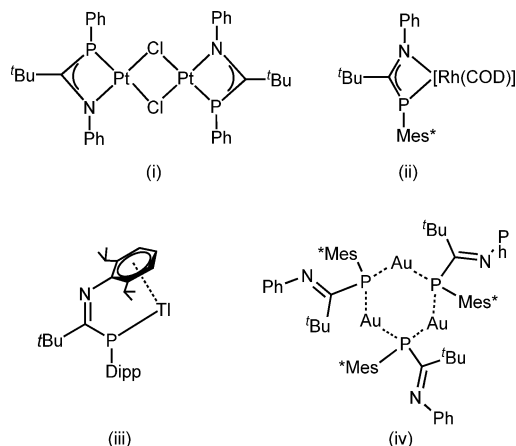
INTRODUCTION

Anionic amidinate ligands, [RNC(R')NR][−], play many important roles in molecular inorganic chemistry. Amidinates have been utilized as chelating ligands in a variety of single site and multimetal catalysis,^{1–9} including examples for polymerization,^{1–4} hydrogenation,⁷ hydroamination,⁵ hydrosilylation,⁸ amidation,⁹ and CO₂ fixation reactions.⁶ In addition to catalysis, the Gordon group has employed amidinate complexes of Ti, V, Mn, Fe, Co, Ni, Cu, Ag, and La as useful precursors for atomic layer deposition.¹⁰ Furthermore, the ability of amidinates to bridge metal ions has provided opportunities to study metal–metal bonding.^{11–13,20}

In contrast, the coordination chemistry of phosphaamidinate analogues, [RNC(R')PR][−], is less well-known since the initial discovery of phosphorus–carbon multiple bond chemistry by Issleib et al. in 1978,¹⁴ and only a few examples of metal phosphaamidinate complexes are reported, including Pt(II) and Rh(I) examples with N,P-chelation,^{14,17} a Ti(I) complex with P,π-aryl-chelation,¹⁶ and a trinuclear-Au(I) complex with μ₂-P bridging.¹⁷ (Chart 1). The coordination chemistry of phosphaamidinates thus far consists of chelation to single metal sites or μ₂-P bridging between two metal sites. Phosphaamidinates possess different electronic properties to that of amidinates, due to the softer P-donor atom and different π-donor behavior of P=C vs N=C multiple bonds. Moreover, additional coordination modes may be available to phosphaamidinates that are unavailable to amidinates. The different electronic features and coordination modes of phosphaamidinates have the potential to complement the established behavior of the prolific amidinate ligands, allowing them to be versatile for designing organometallic architectures.

Our group has been using formamidinates to stabilize unusual tetranuclear copper sulfide clusters that resemble the active site of nitrous oxide reductase.^{18,19} Formamidinates have

Chart 1. Metal Complexes of Phosphaamidinates



been shown to stabilize the 2Cu(I):2Cu(II) and 3Cu(I):1Cu(II) states of a [Cu₄S] model system, but they are unable to stabilize the fully reduced 4Cu(I) state that would model the active state of the enzyme. We hypothesized that the use of phosphaamidinates with mixed P/N-donor atoms in place of harder formamidinates would stabilize a larger range of redox states for our clusters. In an attempt to test our hypothesis, we discovered a new coordination mode of phosphaamidinates that has not been reported before. Herein, we report the synthesis and characterization of hexa- and tetranuclear copper clusters featuring this triply bridging phosphaamidinate coordination mode wherein a single phosphaamidinate unit binds simultaneously to three Cu(I) ions.

Received: May 23, 2018

Scheme 1. Synthesis of Phosphabenzamidine 1 and Phosphabenzamidinate 2

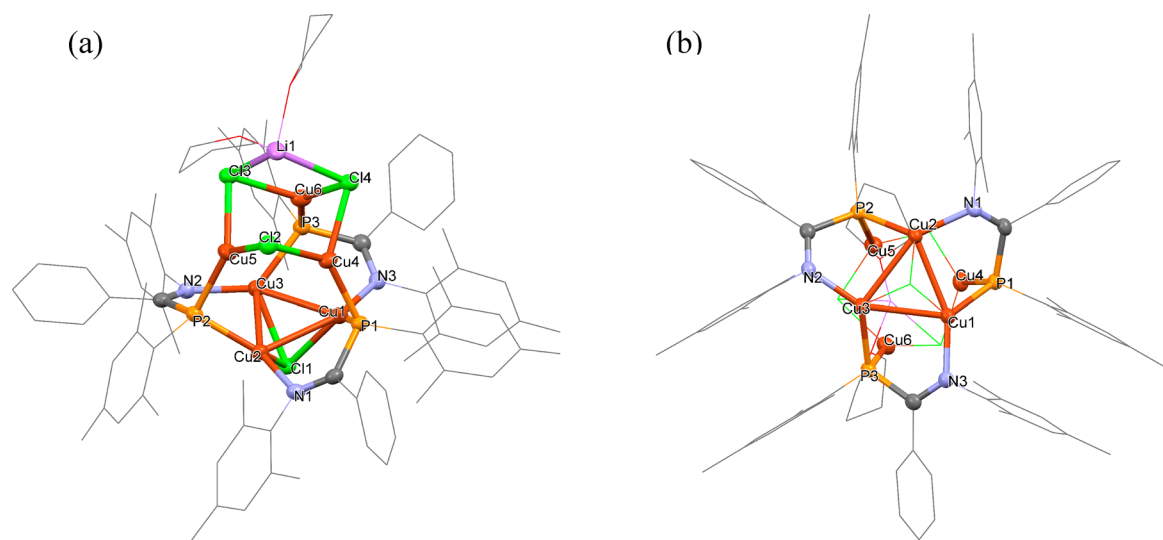
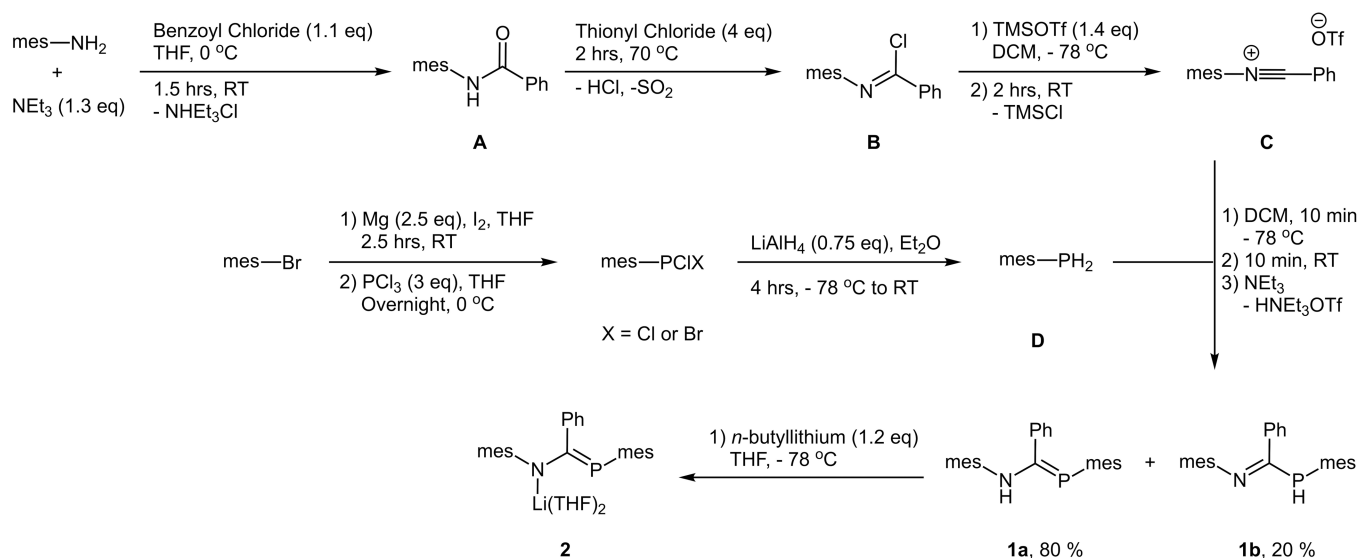


Figure 1. Side (a) and bottom (b) view of the crystal structure of Cu₆[mes-N=C(Ph)-P(mes)]₃Cl₄Li(THF)₂. Only the core structure atoms are shown as 50% probability thermal ellipsoids for clarity.

RESULTS AND DISCUSSION

The phosphabenzamidine **1** was synthesized by adopting the synthetic routes reported in the literature,^{17,21} utilizing *N*-benzylidene-2,4,6-trimethylbenzenaminium triflate (**C**) and mesitylphosphane (**D**) (Scheme 1). The reaction conditions drive a 1,3 hydrogen shift to afford **1a** (~80%) and **1b** (~20%). Without purification, both **1a** and **1b** can be transformed into corresponding lithium phosphabenzamidinate **2** by deprotonation with *n*-butyllithium.

With **2** in hand, we were interested in studying its coordination with Cu(I) ions. Cu(I)Cl was chosen as the source of copper, with the expectation that precipitation of LiCl salt would facilitate coordination. The reaction of **2** with 3 equiv of Cu(I)Cl in THF delivered an orange solid, which showed distinct peaks for inequivalent mesityl CH₃ groups in the ¹H NMR spectrum, possibly due to π - π stacking interactions restricting rotation of the mesityl groups. The crystal structure revealed this orange solid to be Cu₆[mes-N=C(Ph)-P(mes)]₃Cl₄Li(THF)₂ (**3**) (Figure 1). To our surprise,

four Cl⁻ anions and a Li⁺ cation were retained in the structure. We have been unable to induce LiCl precipitation from **3** through a variety of methods, and addition of Na₂S simply results in partial Li⁺/Na⁺ exchange as judged by NMR spectroscopy and preliminary X-ray crystallography.

The solid-state structure of complex **3** consists of two triangular Cu(I) clusters arranged on top of each other as a hexacopper antiprism. The “bottom” Cu1...Cu2...Cu3 base is capped by a Cl⁻ ligand, and the “top” Cu4...Cu5...Cu6 base is supported by three μ_2 -Cl⁻ ligands that, in turn, are capped by a Li⁺ ion. The Li⁺ ion has also two coordinated THF ligands.

The phosphabenzamidinate ligands are arranged in a regular propeller-like chiral fashion, with their N atoms coordinating the “bottom” 3Cu(I) base and their P atoms acting as μ_2 -ligands bridging the “bottom” and “top” bases of the antiprism. The Cu...Cu separations within the “bottom” base are shorter (2.69–2.75 Å) than in the “top” (2.95–3.14 Å), and both are shorter than Cu...Cu separations between the bases (~3.3 Å

for P-bridged Cu(I) ions and 3.6–3.8 Å between nonbridged ones).

Many hexacopper clusters based on either Cu(I) or Cu(II) are reported in the literature, featuring quite different assemblies of Cu atoms (Figure 2).^{24–29} The hexacopper

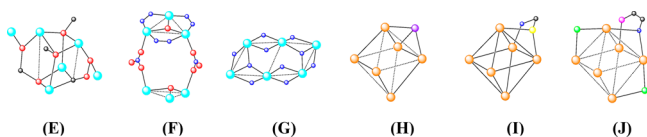


Figure 2. Different assembly types for hexanuclear Cu(I) and Cu(II) clusters. Only core structures are shown for clarity, and only solid lines represent a bond. Aqua ball - Cu(II); orange ball - Cu(I); red ball - O; blue ball - N; gray ball - C; yellow ball - S; pink ball - P; green ball - Cl; purple ball - I.

cluster type E consists of four 5-coordinate Cu(II) atoms located at four alternative vertices of a central defective cubane unit with two μ_3 - and two μ_2 -O atoms, and two satellite Cu(II) atoms connect to the cubane via μ_2 -O atoms.²⁴ The cluster type F consists of two 6-coordinate Cu(II) trimer units bridged by two nitrate ions,²⁵ while G possesses a coplanar assembly of 5-coordinate Cu(II) atoms.²⁶ Octahedral or distorted octahedral assemblies are common for hexanuclear Cu(I) clusters as evidenced by clusters H,²⁷ I,²⁸ and J.²⁹ In contrast, the arrangement of Cu(I) atoms in **3** defines an antiprism rather than an octahedron.

We are interested in more reactive complexes with coordinatively unsaturated Cu(I) ions, as precursors to construct tetranuclear copper sulfide clusters. To attempt to address this, **2** was reacted with 1 and 2 equiv of Cu(I)Cl, to target a di- or trinuclear cluster with a 1:1 ratio of bidentate phosphabenzamidinate to Cu(I). Interestingly, the ³¹P NMR spectra showed formation of **3** and unreacted **2** in both reactions, suggesting that the formation of **3** is highly favorable regardless of metal:ligand stoichiometry in the reaction mixture.

As confirmed by the crystal structure, the presence of μ_2 -Cl ligands stabilizes **3** by balancing the charge and saturating the Cu centers. Such coordination of halides is common, and a similar coordination has been reported by Jessop and co-workers in a phosphamidinate-Cu(I)Br cluster.²³ So, we next wondered whether a more reactive complex could be attained by applying a halide-free copper source. Mesitylcopper was an ideal candidate for this purpose, as it allows the simultaneous deprotonation and coordination. To begin with, **1** was reacted with 1 equiv of mesitylcopper at room temperature, and after 3 h, **1** was partially consumed and a new product was observed by ³¹P NMR spectroscopy. The formation of mesitylene was confirmed by ¹H NMR spectroscopy. After purification, the ¹H

NMR spectrum of the new species indicated restricted rotation of the mesityl groups, similar to **3**. However, the solubility of the new species was poor in most of the available solvents, hence making it is difficult to grow X-ray quality crystals or analyze the structure by solution methods.

Next, phosphoramidinate **4** was synthesized and applied in place of **1**. The previous synthetic route (Scheme 1) could not be applied as multiple attempts to make the imido chloride that corresponds to (B) were unsuccessful. Hence, ethyl-*N*-mesitylformimidate was synthesized²² and reacted with lithium mesitylhydrophosphanide to afford **4** as a yellow green solid (Scheme 2). Production of mesityl phosphane was also observed as the lithium mesitylhydrophosphanide is basic enough to deprotonate **4**. However, an overnight long reaction time, followed by the addition of NH₄Cl, shifted the equilibrium toward the formation of **4**.

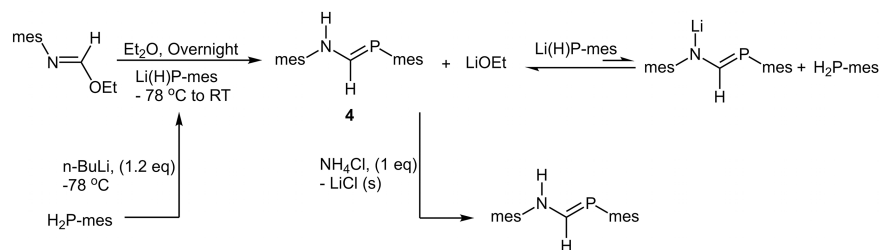
A small-scale reaction of **4** (0.0673 mmol) with mesitylcopper in Et₂O afforded **5** as an orange solid after 2 days. However, scaling up the reaction by 10 times required 8 days to complete. So, an alternative approach was applied by first deprotonating **4** with sodium bis(trimethylsilyl)amide (NaHMDS) and then adding Cu(MeCN)₄PF₆ in Et₂O, resulting in rapid formation of **5**. The ¹H NMR spectrum of **5** exhibited restricted mesityl bond rotation similar to **3**, and the single crystal XRD confirmed the identity of **5** as Cu₄(mes-N=CH-P-mes)₄ (Figure 3).

The structure of **5** contains a tetrahedron of Cu(I) ions, with the overall cluster having noncrystallographic S₄ symmetry. Each ligand caps one of the faces of the tetrahedron with N atoms reaching the Cu atom opposite to the bridged edge at a 2.01 Å distance. All P–Cu bond lengths are in a narrow range 2.26–2.28 Å and have an average Cu...Cu separation 2.94 Å. The two opposite nonbridged Cu atoms are elongated to a distance of 3.13 Å.

The literature includes reports of a variety of tetranuclear Cu(II) and Cu(I) assemblies. The Cu(II) structures include chairlike K,³⁰ linear L,³¹ tetrahedral M,³² and planar N³³ geometries (Figure 4). Most of them are held together by bridging O or N atoms. Tetrahedral or distorted tetrahedral assemblies are common for tetranuclear Cu(I) clusters, yet different arrangements are possible, as evidenced by P³⁵ where four planar Cu(I) atoms are bridged by carboxylate ligands above and below the plane. Both O and Q display tetrahedral arrangements of Cu(I) atoms. Each face of O is occupied by a μ_3 -I atom, and each edge of Q is bridged by a μ_2 -Se atom.^{34,36} Complex **5** also resembles a tetrahedron of Cu(I) ions and is similar to O, with each face capped by a phosphoramidinate ligand.

Even in the absence of halides, **5** still has μ_2 -bridging phosphorus atoms, implying that the triply bridging coordination behavior of phosphoramidates is intrinsic. To our

Scheme 2. Synthesis of *N*-((Mesitylphosphanylidene)methyl)-2,4,6-trimethylaniline



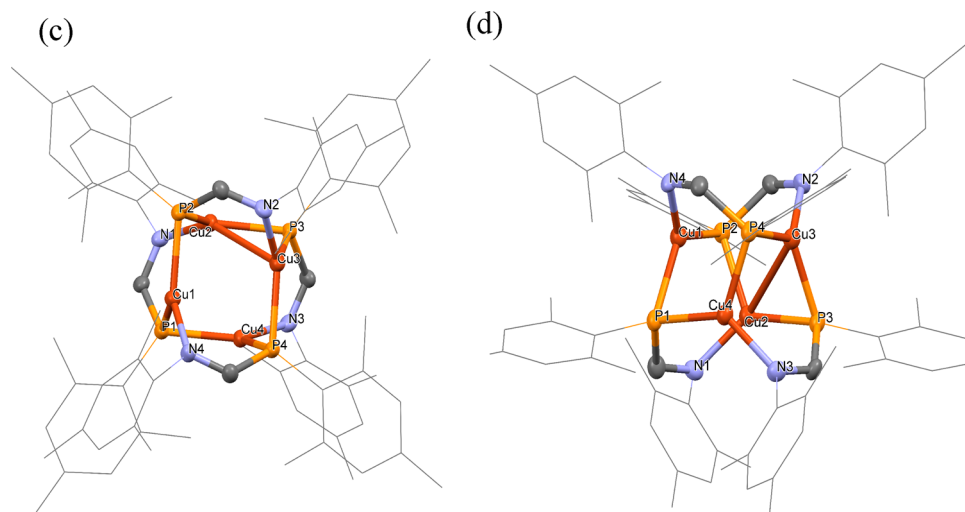


Figure 3. Top (a) and side (b) view of the crystal structure of $\text{Cu}_4[\text{mes-N}=\text{CH-P-mes}]_4$. Only the core structure atoms are shown as 50% probability thermal ellipsoids for clarity.

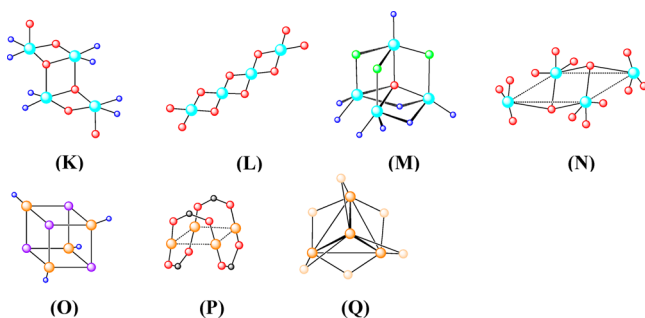
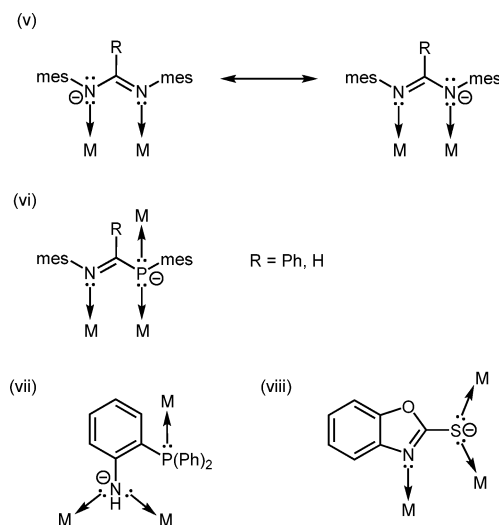


Figure 4. Different assembly types for tetranuclear Cu(I) and Cu(II) clusters. Only core structures are shown for clarity, and only solid lines represent a bond. Aqua ball - Cu(II); orange ball - Cu(I); red ball - O; blue ball - N; gray ball - C; yellow ball - S; pink ball - P; green ball - Cl; purple ball - I; beige ball - Se.

knowledge, this coordination mode has not been observed previously in the phosphamidinate literature. Analogous behavior is not seen in formamidinates, as the nitrogen lone pairs are resonance delocalized and thus unavailable to bridge two metals at a single N atom (Chart 2). In conjugate bases of **1** and **4**, there is apparently less delocalization due to poor overlap of the 3p orbitals of P with the 2p orbitals of C, making the phosphorus lone pairs available for an extra coordination to a third metal center.

However, phosphamidinates do not coordinate to Au(I) in a similar fashion. The Lammertsma group reported two coordination complexes of phosphamidinates with Rh(I) and Au(I).¹⁷ In the Rh(I) complex, the phosphamidinate ligand chelates to a single Rh(I) center, whereas the Au(I) complex displays μ_2 -P, bridging without any N-coordination (Chart 1 (ii), (iv)). This behavior is likely driven by the preference of Au(I) to have linear coordination geometry, and so phosphamidinate ligands are more likely to exhibit triply bridging coordination behavior with Cu ions (Chart 2). A 2D network of Cu(II) atoms supported by a μ_3 -bridging tridentate carboxylate has been reported,³⁷ and the mode of coordination is attributed to the electronic effects of the substituents. In addition, the reaction of $\text{Cu}(\text{O}_2\text{CPh})_2 \cdot 2\text{H}_2\text{O}$ with a mixture of $(\text{py})_2\text{CO}$ and NaN_3 produced a hexanuclear Cu(II) cluster supported by $(\text{py})_2\text{CO}_2^{2-}$ and $(\text{py})_2\text{C}(\text{OH})\text{O}^-$ anionic ligands

Chart 2. Coordination Modes of Deprotonated NN, NP, and NS Ligands



having μ_2 -O bridging two Cu atoms and each nitrogen coordinating to a different Cu atom.²⁴ The (2-(diphenylphosphanyl)phenyl)amide ligand (vii) is an example of a 1,1,4-N,P ligand, stabilizing **J** (Figure 4) but with μ_2 -N rather than μ_2 -P bridges. Benzoxazole-2-thiolate (viii) possesses a very similar coordination to that of phosphamidinates discussed here. Ligand (viii) acts as 1,1,3-S,N ligand stabilizing **I** (Figure 4) with μ_2 -S bridging to two Cu(I) atoms and N coordinating to a different Cu(I) atom. The extra coordination in both (vii) and (viii) has been generated at the site of deprotonation (amide and thiolate groups, respectively), whereas the deprotonation of the amine group in **1** and **4** leads to the formation of a $\text{N}=\text{C}$ bond and creates an extra coordination at P.

The redox behavior of both **3** and **5** was studied using cyclic voltammetry. Complex **3** displayed few redox events that are not well-defined, and surprisingly, complex **5** was redox innocent (see the Supporting Information, page S9) despite being supported by electron rich phosphorus σ -donors. In addition, due to our interest in constructing tetranuclear copper-sulfide clusters, we added several sulfur-atom donor

reagents to **5**. Unfortunately, no reaction was observed under the conditions we examined, indicating the inert nature of **5** (which is even air-stable).

CONCLUSION

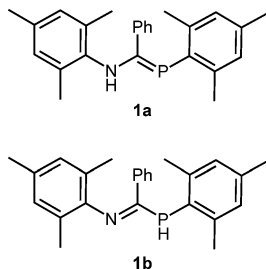
In summary, phosphamidine ligands **1** and **4** have been synthesized and characterized. The corresponding phosphamidinates coordinate with Cu(I)Cl and Cu(MeCN)₄PF₆, respectively, making complexes **3** and **5**. As evidenced by the crystal structures, phosphamidinates coordinate to Cu(I) in triply bridging fashion with the help of μ_2 -bridging P-donor atoms. This observation exemplifies the different coordination behavior of phosphamidinates compared to that of isoelectronic amidinates. Neither **3** nor **5** exhibits any well-defined redox chemistry; nevertheless, we believe the new coordination mode for phosphamidinate ligands will enhance their utilization in building organometallic architectures.

EXPERIMENTAL SECTION

General Remarks. Unless otherwise mentioned, all the syntheses were done in a glovebox filled with N₂ or using standard Schlenk line techniques. All the chemicals purchased from a commercial source were used without further purification. Solvents were dried using a glass contour solvent system built by Pure Process Technology, LLC. Deuterated solvents that were packed under Ar were stored in 3-Å molecular sieves without further degassing. Compounds **A**, **B**, **C**, **D**, and **E** were synthesized by adopting synthetic routes reported in the literature.^{15,16,21} **Caution!** Synthesis of **D** involves quenching LiAlH₄ with H₂O. Extreme care should be taken when adding the first few drops of H₂O, as the quenching is highly exothermic and H₂ is evolved. Any waste or glassware containing phosphane **D** should be properly cleaned as phosphanes are highly smelly.

Instrumentation. ³¹P NMR spectra were recorded at ambient temperature using a Bruker Avance DPX-400 MHz instrument. All the ¹H NMR spectra were recorded at ambient temperature using either Bruker Avance DPX-400 or Bruker Avance DPX-500 MHz instruments. Mass analyses were performed with an Advion Expression¹ CMS mass spectrometer using APCI⁺ mode. Elemental analyses were performed by the Midwest Microlab, LLC, in Indianapolis, IN. X-ray crystallography data of complexes **3** and **5** were collected at the X-ray Structural Laboratory at Marquette University (Milwaukee, WI) using a SuperNova, Dual, Cu at home/near, Atlas diffractometer [Cu K α (λ = 1.54184)] at 100.15 K. The structure was solved with the Olex2 structure solution program using Charge Flipping and refined with the ShelXL refinement package using Least Squares minimization. Electrochemical data of both **3** and **5** (approximately 1 mmol in THF) were collected in a classic three-electrode system: a Pt working electrode, a Pt counter electrode, and a Ag/Ag⁺ reference electrode, using a WaveNow USB Potentiostat from Pine Research Instrumentation.

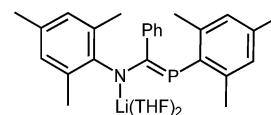
Synthesis of *N*-((Mesitylphosphanylidene)(phenyl)methyl)-2,4,6-trimethylaniline (1**).**



A solution of 2,4,6-trimethylphenylphosphane (0.2500 g, 1.64 mmol) in DCM (2 mL) was added dropwise to a suspension of *N*-benzylidene-2,4,6-trimethylbenzenaminium trifluoromethanesulfonate (0.6101 g, 1.64 mmol) in DCM (2.5 mL) at -78°C . The reaction

mixture was stirred for 10 min at -78°C , and the cooling bath was removed. The mixture was further stirred for 30 min, while allowing it to warm up to the room temperature. Triethylamine (252 μL , 1.80 mmol) was added, and the color of the solution changed from red-orange to yellow. The mixture was stirred for 15 min, and volatiles were removed under vacuum, leaving a yellow-orange oily residue. It was purified (under normal atmosphere) by filtering over a pad of neutral, activated alumina eluting with pentane. Volatiles were removed under vacuum, leaving (**1**) as a yellow solid. The gram scale synthesis gave (**1**) as a yellow sticky product which solidified in weeks. Reaction conditions yield **1** as a mixture of **1a** (~80%) and **1b** (~20%). Total yield: 0.3506 g, 72%. ¹H NMR of **1a** (500 MHz, CDCl₃) δ 7.34 (d, J = 8.2 Hz, 2H), 7.21 (t, J = 7.3 Hz, 1H), 7.14 (t, J = 7.5 Hz, 2H), 6.99 (s, 2H), 6.67 (s, 2H), 6.17 (s, 1H), 2.59 (s, 6H), 2.29 (s, 3H), 2.15 (s, 3H), 2.04 (s, 6H). ³¹P NMR of **1a** (162 MHz, CDCl₃) δ 61.74 (s), **1b** (162 MHz, CDCl₃) δ -74.51 (d, J = 241.1 Hz). m/z theoretical: 373.20, 374.20, 375.20. Found 374.3, 375.3, 376.3

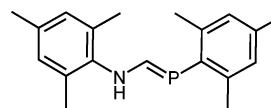
Synthesis of Bis(tetrahydrofuran)lithium mesityl((mesitylphosphanylidene)(phenyl)methyl)amide (2**).**



n-Butyllithium (12.5 mL of 1.6 M in hexanes, 19.9 mmol) was added dropwise to a solution of (**1**) (4.9544 g, 16.6 mmol) in THF (25 mL) at -78°C . The color of the mixture was changed from yellow to orange to dark brown. The resulting mixture was allowed to warm up to room temperature and stirred for a further 10 min. The volatiles were removed under vacuum, leaving a brown residue, which was dissolved in a minimum amount of THF and kept at -20°C to afford (**2**) as an orange solid. It was filtered and washed with cold pentane. The filtrate was completely evaporated and redissolved in a minimum amount of THF and kept at -20°C to afford a second crop. A third crop was obtained in a similar way. Total yield: 5.3342 g, 61%. ¹H NMR (400 MHz, THF-*d*8) δ 7.21–7.12 (m, 2H), 6.86–6.79 (m, 3H), 6.75 (s, 2H), 6.41 (s, 2H), 3.64–3.59 (m, 4H; THF), 2.40 (s, 6H), 2.28 (s, 6H), 2.21 (s, 3H), 1.99 (s, 3H), 1.79–1.74 (m, 4H; THF). ³¹P NMR (162 MHz, THF-*d*8) δ 25.55 (s).

Synthesis of Cu₆[mes-N=C(Ph)-P-mes]₃Cl₄Li(THF)₂ (3**).** A solution of (**2**) (0.1014 g, 0.19 mmol) in THF (3 mL) was added dropwise to a suspension of CuCl (0.0575 g, 0.58 mmol) in THF (5 mL) over 10 min. The reaction mixture immediately changed to yellow and to cloudy orange at the end of the slow addition. It was stirred at room temperature for 1 h and filtered through a pad of Celite. The filtrate was completely evaporated, leaving a yellow solid. It was added with DCM (6 mL) and filtered through a pad of Celite to remove insoluble LiCl. The Celite pad was washed with DCM (1 mL \times 2). The filtrate was completely evaporated, leaving (**3**) as a yellow-orange solid. Yield: 0.0890 g, 77%. X-ray quality crystals were grown by cooling a saturated solution of (**3**) in THF at -20°C . ¹H NMR (400 MHz, CDCl₃) δ 6.97 (s, 2H), 6.82 (t, J = 7.2 Hz, 1H), 6.75 (t, J = 7.5 Hz, 2H), 6.65 (s, 1H), 6.62 (s, 1H), 5.86 (s, 1H), 5.62 (s, 1H), 3.77 (s, 4H; THF), 3.03 (s, 3H), 2.60 (s, 3H), 1.99 (s, 3H), 1.98 (s, 3H), 1.97 (s, 3H), 1.86 (s, 8H; THF), 1.19 (s, 3H). ³¹P NMR (162 MHz, CDCl₃) δ -61.95 (s). Anal. Calcd For C₈₃H₉₇Cu₆Cl₄LiO₂P₃: C, 55.64; H, 5.46; N, 2.35. Found: C, 54.92; H, 5.12; N, 2.04. (the error of % C was greater than the limit of satisfactory due to the solvent coordination).

Synthesis of *N*-((Mesitylphosphanylidene)methyl)-2,4,6-trimethylaniline (4**).**



n-Butyllithium (1.6 M solution in hexane, 4.9 mL, 7.86 mmol) was added dropwise over 15 min to a solution of 2,4,6-trimethylphenylphosphane (1.0000 g, 6.57 mmol) in Et₂O (45 mL) at -78°C . The

resulting mixture was stirred for 30 min at the same temperature, followed by another 30 min outside the cold well, allowing it to warm up to room temperature to afford lithium 2,4,6-trimethylphenyl-hydrophosphanide as a yellow cloudy solution. It was added dropwise over 30 min to a solution of ethyl *N*-mesitylformimidate (1.2569 g, 6.57 mmol) in Et₂O (10 mL) at -78°C . The resulting mixture was stirred for 30 min at the same temperature and allowed to warm up to room temperature overnight. The resulting yellow solution was added with solid NH₄Cl (0.3515 g, 6.57 mmol) and stirred for 30 min and then filtered through a pad of Celite to remove the insoluble LiCl. The filtrate was completely evaporated, leaving a yellow solid which was added with pentane (20–25 mL) and filtered off using a coarse frit and washed with pentane (2 mL \times 6) to afford (4) as a yellow-green solid. (If any unreacted ethyl *N*-mesitylformimidate or 2,4,6-trimethylphenylphosphane is present, the yellow solid which results from complete evaporation of the filtrate will appear as wet and sticky. In that case, washing with pentane will remove any unreacted materials and the byproducts, leaving (4) as a dry solid.) Yield: 1.0161 g, 52%. ¹H NMR (400 MHz, C₆D₆) δ 7.63 (dd, *J* = 44.1, 13.9 Hz, 1H), 6.88 (s, 2H), 6.54 (s, 2H), 2.61 (s, 6H), 2.15 (s, 3H), 2.05 (s, 3H), 1.89 (s, 6H). ³¹P NMR (162 MHz, C₆D₆) δ 54.43 (d, *J* = 44.2 Hz). *m/z* theoretical: 297.16, 298.17, 299.17. Found: 298.4, 299.4, 300.4.

Synthesis of Cu₄[mes-N=CH-P-mes]₄ (5) Using Mesitylcopper. A solution of mesitylcopper (0.1342 g, 0.73 mmol) in Et₂O (11 mL) was added dropwise over 20 min to a solution of (4) (0.2184 g, 0.73 mmol) in Et₂O (12 mL). The reaction mixture was well capped and stirred at 40°C for 3 h. The ³¹P NMR of an aliquot showed the complete consumption of (4) to multiplets around -55 to -80 ppm. The reaction mixture was further stirred for 8 days at 40°C , resulting in a yellow precipitate. The precipitate was collected by filtration and redissolved in benzene and filtered off through a pad of Celite to remove a brown color byproduct (possibly decomposed Cu from mesitylcopper). The resulting yellow-orange filtrate was completely evaporated, leaving 5 as a yellow-orange solid. Yield: 0.1728 g, 65%. ¹H NMR (400 MHz, C₆D₆) δ 8.38 (s, 1H), 6.87 (s, 1H), 6.84 (s, 1H), 6.78 (s, 1H), 6.55 (s, 1H), 2.92 (s, 3H), 2.53 (s, 3H), 2.50 (s, 3H), 2.17 (s, 3H), 2.08 (s, 3H), 1.53 (s, 3H). ³¹P NMR (162 MHz, C₆D₆) δ -74.39 (s). Anal. Calcd For C₇₆H₉₂Cu₄N₄P₄: C, 63.41; H, 6.44; N, 3.89. Found: C, 61.53; H, 6.32; N, 3.60. (Repeated attempts gave consistent results, implying incomplete combustion.)

Synthesis of (5) Using Cu(MeCN)₄PF₆. (4) (0.1771 g, 5.96 mmol) and NaHMDS (0.1201 g, 6.55 mmol) were mixed in Et₂O (8 mL) and stirred for 1 h at room temperature. Cu(MeCN)₄PF₆ (0.2220 g, 5.96 mmol) was added as a solid to the reaction mixture. It was crushed using a glass rod, while it is inside the reaction mixture, as the solubility of Cu(MeCN)₄PF₆ in Et₂O is poor. Immediate formation of an orange solid was seen. The reaction mixture was further stirred at room temperature for 3 h and filtered off to get an orange solid which was washed with pentane (2 mL \times 3). This solid was redissolved in benzene (15 mL) and stirred for 10–15 min. Then it was filtered through a pad of Celite, and the Celite was washed with benzene (2 mL \times 6). The filtrate was completely evaporated to afford (5) as an orange solid. X-ray quality crystals were grown by slow evaporation of a concentrated solution of 5 in a 1:1 mixture of toluene and benzene. Yield: 0.1534 g, 72%. ¹H NMR (400 MHz, C₆D₆) δ 8.38 (s, 1H), 6.87 (s, 1H), 6.84 (s, 1H), 6.78 (s, 1H), 6.55 (s, 1H), 2.92 (s, 3H), 2.53 (s, 3H), 2.50 (s, 3H), 2.17 (s, 3H), 2.08 (s, 3H), 1.53 (s, 3H). ³¹P NMR (162 MHz, C₆D₆) δ -74.39 (s). Anal. Calcd For C₇₆H₉₂Cu₄N₄P₄: C, 63.41; H, 6.44; N, 3.89. Found: C, 61.04, H, 6.30; N, 3.44. (Repeated attempts gave consistent results, implying incomplete combustion.)

■ ASSOCIATED CONTENT

■ Supporting Information

The Supporting Information is available free of charge on the ACS Publications website at DOI: 10.1021/acs.inorgchem.8b01422.

NMR spectra, mass spectra, electrochemistry data (PDF)

■ Accession Codes

CCDC 1845805 and 1845806 contain the supplementary crystallographic data for this paper. These data can be obtained free of charge via www.ccdc.cam.ac.uk/data_request/cif, or by emailing data_request@ccdc.cam.ac.uk, or by contacting The Cambridge Crystallographic Data Centre, 12 Union Road, Cambridge CB2 1EZ, UK; fax: +44 1223 336033.

■ AUTHOR INFORMATION

■ Corresponding Author

*E-mail: npm@uic.edu.

■ ORCID

Neal P. Mankad: 0000-0001-6923-5164

■ Notes

The authors declare no competing financial interest.

■ ACKNOWLEDGMENTS

The National Institutes of Health (R01 GM116820) provided financial support.

■ REFERENCES

- (1) Coles, M. P.; Jordan, R. F. Cationic Aluminum Alkyl Complexes Incorporating Amidinate Ligands. Transition-Metal-Free Ethylene Polymerization Catalysts. *J. Am. Chem. Soc.* **1997**, *119*, 8125–8126.
- (2) Shibayama, K. The Polymerization of Methyl Methacrylate Using Cu(II) Benzamidinate Complexes. *Polym. J.* **2003**, *35*, 711–713.
- (3) Li, W.; Bai, S.-D.; Su, F.; Yuan, S.-F.; Duan, X.-E.; Liu, D.-S. Zirconium complexes based on an ethylene linked amidinate–amido ligand: synthesis, characterization and ethylene polymerization. *New J. Chem.* **2017**, *41*, 661–670.
- (4) Luo, Y.; Lei, Y.; Fan, S.; Wang, Y.; Chen, J. Synthesis of mono-amidinate-ligated rare-earth-metal bis(silylamide) complexes and their reactivity with [Ph₃C][B(C₆F₅)₄], AlMe₃ and isoprene. *Dalton Trans.* **2013**, *42*, 4040–4051.
- (5) Brunner, T. S.; Benndorf, P.; Gamer, M. T.; Knöfel, N.; Gugau, K.; Roesky, P. W. Enantiopure Amidinate Complexes of the Rare-Earth Elements. *Organometallics* **2016**, *35*, 3474–3487.
- (6) Meléndez, D. O.; Lara-Sánchez, A.; Martínez, J.; Wu, X.; Otero, A.; Castro-Osma, J. A.; North, M.; Rojas, R. S. Amidinate Aluminum Complexes as Catalysts for Carbon Dioxide Fixation into Cyclic Carbonates. *ChemCatChem* **2018**, *10*, 2271–2277.
- (7) Martínez-Prieto, L. M.; Cano, I.; Márquez, A.; Baquero, E. A.; Tricard, S.; Cusinato, L.; del Rosal, I.; Poteau, R.; Coppel, Y.; Philippot, K.; Chaudret, B.; Cámpora, J.; van Leeuwen, P. W. N. M. Zwitterionic amidinates as effective ligands for platinum nanoparticle hydrogenation catalysts. *Chem. Sci.* **2017**, *8*, 2931–2941.
- (8) Ge, S.; Meetsma, A.; Hessen, B. Highly Efficient Hydrosilylation of Alkenes by Organoyttrium Catalysts with Sterically Demanding Amidinate and Guanidinate Ligands. *Organometallics* **2008**, *27*, 3131–3135.
- (9) Wang, J.; Li, J.; Xu, F.; Shen, Q. Anionic Bridged Bis(amidinate) Lithium Lanthanide Complexes: Efficient Bimetallic Catalysis for Mild Amidation of Aldehydes with amines. *Adv. Synth. Catal.* **2009**, *351*, 1363–1370.
- (10) Lim, B. S.; Rahtu, A.; Park, J.-S.; Gordon, R. G. Synthesis and Characterization of Volatile, Thermally Stable, Reactive Transition Metal Amidinates. *Inorg. Chem.* **2003**, *42*, 7951–7958.
- (11) Cotton, F. A.; Walton, R. A. *Multiple Bonds between Metal Atoms*, 2nd ed.; Oxford University Press: New York, 1993.
- (12) Barker, J.; Kilner, M. The coordination chemistry of the amidine ligand. *Coord. Chem. Rev.* **1994**, *133*, 219–291.

- (13) Mohamed, A. A.; Abdou, H. E.; Irwin, M. D.; López-De-Luzuriaga, J. M.; Fackler, J. P., Jr. Gold(I) Formamidinate Clusters: The Structure, Luminescence, and Electrochemistry of the Tetranuclear, Base-Free $[\text{Au}_4(\text{ArNC}(\text{H})\text{NAr})_4]$. *J. Cluster Sci.* **2003**, *14*, 253–266.
- (14) Issleib, K.; Schmidt, H.; Meyer, H. Phospha-amidine. *J. Organomet. Chem.* **1978**, *160*, 47–57.
- (15) Boéré, R. T.; Cole, M. L.; Junk, P. C.; Masuda, J. D.; Wolmershäuser, G. An N,P-disubstituted-2-aminophosphaalkene and Lithium and Potassium Complexes of the Deprotonated Anion “Phosphaamidinate”. *Chem. Commun.* **2004**, No. 22, 2564–2565.
- (16) Li, X.; Song, H.; Cui, C. Azaphosphaallyl Anion lithium $[\text{ArNC}(\text{But})\text{PAr}]\text{-Li}^+(\text{THF})_4$ and Its Monomeric Potassium and Thallium Complexes (Ar = 2,6-*iPr*2C6H3). *Dalton Trans.* **2009**, No. 44, 9728–9730.
- (17) Van Dijk, T.; Burck, S.; Rong, M. K.; Rosenthal, A. J.; Nieger, M.; Slootweg, J. C.; Lammertsma, K. Facile Synthesis of Phosphaamidines and Phosphaamidines using Nitrilium Ions as an Imine Synthons. *Angew. Chem.* **2014**, *126*, 9214–9217.
- (18) Johnson, B. J.; Antholine, W. E.; Lindeman, S. V.; Mankad, N. P. A Cu4S Model for the Nitrous Oxide Reductase Active Sites Supported Only by Nitrogen Ligands. *Chem. Commun.* **2015**, *51*, 11860–11863.
- (19) Johnson, B. J.; Antholine, W. E.; Lindeman, S. V.; Graham, M. J.; Mankad, N. P. A One-Hole Cu4S Cluster with N2O Reductase Activity: A Structural and Functional Model for CuZ*. *J. Am. Chem. Soc.* **2016**, *138*, 13107–13110.
- (20) Cotton, F. A.; Donahue, J. P.; Hall, M. B.; Murillo, C. A.; Villagrán, D. Reaction Products of $\text{W}(\text{CO})_6$ with Formamidines; Electronic Structure of a $\text{W}_2(\mu\text{-CO})_2$ Core with Unsymmetric Bridging Carbonyls. *Inorg. Chem.* **2004**, *43*, 6954–6964.
- (21) Takeda, Y.; Nishida, T.; Minakata, S. 2,6-Diphospha-s-indacene-1,3,5,7(2 H,6 H)-tetraone: A Phosphorus Analogue of Aromatic Diimides with the Minimal Core Exhibiting High Electron-Accepting Ability. *Chem. - Eur. J.* **2014**, *20*, 10266–10270.
- (22) Song, M.; Donnadiou, B.; Soleilhavoup, M.; Bertrand, G. Synthesis of Phosphaformamidines and Phosphaformamidates. *Chem. - Asian J.* **2007**, *2* (7), 904–908.
- (23) Kandel, R.; Huynh, K.; Dalglish, L.; Wang, R.; Jessop, P. G. Contrasting Connectivity of Amidine and Phosphaamidine (1,3-P,N) Cu(I) Complexes. *Inorg. Chim. Acta* **2016**, *445*, 117–123.
- (24) Stamatatos, T. C.; Vlahopoulou, J. C.; Tanguolis, V.; Raptopoulou, C. P.; Terzis, A.; Papaefstathiou, G. S.; Perlepes, S. P. New Copper(II) Clusters and Coordination Polymers from the Amalgamation of Azide/Benzoate/di-2-pyridyl ketone Ligands. *Polyhedron* **2009**, *28*, 1656–1663.
- (25) Sakai, K.; Yamada, Y.; Tsubomura, T.; Yabuki, M.; Yamaguchi, M. Synthesis, Crystal Structure, and Solution Properties of a Hexacopper(II) Complex with Bridging Hydroxides, Pyrazolates, and Nitrates. *Inorg. Chem.* **1996**, *35*, 542–544.
- (26) Gu, Z.-G.; Xu, Y.-F.; Yin, X.-J.; Zhou, X.-H.; Zuo, J.-L.; You, X.-Z. Cluster-based Copper(II) Coordination Polymers with Azido Bridges and Chiral Magnets. *Dalton Trans.* **2008**, No. 41, 5593–5602.
- (27) Jaros, S. W.; Sokolnicki, J.; Wołoszyn, A.; Haukka, M.; Kirillov, A. M.; Smoleński, P. A Novel 2D Coordination Network Built from Hexacopper(I)-iodide Clusters and Cage-like Aminophosphine Blocks for Reversible “turn-on” Sensing of Aniline. *J. Mater. Chem. C* **2018**, *6*, 1670–1678.
- (28) Gao, X.; He, S.; Zhang, C.; Du, C.; Chen, X.; Xing, W.; Chen, S.; Clayborne, A.; Chen, W. Single Crystal Sub-Nanometer Sized $\text{Cu}_6(\text{SR})_6$ Clusters: Structure, Photophysical Properties, and Electrochemical Sensing. *Adv. Sci.* **2016**, *3*, 1600126.
- (29) Liebing, P.; Freudenberg, J.; Heiser, C.; Merzweiler, K. Z. Novel Copper(I) Clusters with 2-(Diphenylphosphanyl)anilide Ligands. Synthesis and Crystal Structures of $[\text{Cu}_6 \times 2(\text{NHR})_4]$ (X = Cl, Br, I; R = C6H4–2-PPh2). *Z. Anorg. Allg. Chem.* **2017**, *643*, 203–208.
- (30) Li, X.; Cheng, D.; Lin, J.; Li, Z.; Zheng, Y. Di-, Tetra-, and Hexanuclear Hydroxy-Bridged Copper(II) Cluster Compounds: Syntheses, Structures, and Properties. *Cryst. Growth Des.* **2008**, *8*, 2853–2861.
- (31) Fairbairn, R. E.; Mclellan, R.; McIntosh, R. D.; Palacios, M. A.; Brechin, E. K.; Dalgarno, S. J. Oxacalix[4]arene-Supported di-, tetra- and Undecanuclear Copper(II) Clusters. *Dalton Trans.* **2014**, *43*, 5292–5298.
- (32) Chiarella, G. M.; Melgarejo, D. Y.; Prosvirin, A. V.; Dunbar, K. R.; Fackler, J. P. Tetranuclear, Oxygen Centered Copper(II) Clusters Linked Together with Guanidine-Guanidinate Ligands. *J. Cluster Sci.* **2010**, *21*, 551–565.
- (33) Li, H. J.; Zhang, E. P.; Guo, Q. Q.; Hou, H. W.; Fan, Y. T. Structure and Magnetism of a Porous Three-dimensional Metal-organic Framework Based on Planar Tetranuclear Copper(II) Cluster Units. *Sci. China: Chem.* **2010**, *53*, 2118–2122.
- (34) Kyle, K. R.; Ryu, C. K.; Ford, P. C.; Dibeneditto, J. A. Photophysical Studies in Solution of the Tetranuclear Copper(I) Clusters $\text{Cu}_4\text{L}_4\text{L}_4$ (L = Pyridine or Substituted Pyridine). *J. Am. Chem. Soc.* **1991**, *113*, 2954–2965.
- (35) Sevryugina, Y.; Hietsoi, O.; Petrukhina, M. A. Tetranuclear Copper(I) Clusters: Impact of Bridging Carboxylate Ligands on Solid State Structure and Photoluminescence. *Chem. Commun.* **2007**, No. 37, 3853–3855.
- (36) Jin, X.; Tang, K.; Long, Y.; Tang, Y. A Tetranuclear Copper(I) Cluster Complex with a Benzeneselenolate Ligand, $(\text{Me}_4\text{N})_2[\text{Cu}_4(\text{SePh})_6]\cdot\text{CH}_3\text{OH}$. *Acta Crystallogr., Sect. C: Cryst. Struct. Commun.* **1999**, *55*, 1799–1800.
- (37) Yang, L.; Zhang, S.; Liu, X.; Yang, Q.; Wei, Q.; Xie, G.; Chen, S. Effect of Phenylacetic Acid Coligands on the Structures and Magnetic Properties of Azido-bridged Copper(ii)-chain Compounds. *CrystEngComm* **2014**, *16*, 4194–4201.